

Cervical MUC5B and MUC5AC are Barriers to Ascending Pathogens During Pregnancy

Yusuke Ueda,¹ Haruta Mogami,¹  Yosuke Kawamura,¹ Masahito Takakura,¹ Asako Inohaya,¹ Eriko Yasuda,¹ Yu Matsuzaka,¹ Yoshitsugu Chigusa,¹ Shinji Ito,² Masaki Mandai,¹ and Eiji Kondoh¹

¹Department of Gynecology and Obstetrics, Kyoto University Graduate School of Medicine, 54 Shogoin-kawahara-cho, Sakyo-ku, Kyoto 606-8507, Japan

²Medical Research Support Center, Graduate School of Medicine, Kyoto University, Yoshida-Konoe-cho, Sakyo-ku, Kyoto 606-8501, Japan

Correspondence: Haruta Mogami, MD, PhD, Department of Gynecology and Obstetrics, Kyoto University Graduate School of Medicine, 54 Shogoin Kawahara-cho, Sakyo-ku, Kyoto 606-8507, Japan. Email: mogami@kuhp.kyoto-u.ac.jp.

Abstract

Context: Cervical excision is a risk factor for preterm birth. This suggests that the cervix plays an essential role in the maintenance of pregnancy.

Objective: We investigated the role of the cervix through proteomic analysis of cervicovaginal fluid (CVF) from pregnant women after trachelectomy surgery, the natural model of a lack of cervix.

Methods: The proteome compositions of CVF in pregnant women after trachelectomy were compared with those in control pregnant women by liquid chromatography–tandem mass spectrometry and label-free relative quantification. MUC5B/AC expression in the human and murine cervixes was analyzed by immunohistochemistry. Regulation of MUC5B/AC expression by sex steroids was assessed in primary human cervical epithelial cells. In a pregnant mouse model of ascending infection, *Escherichia coli* or phosphate-buffered saline was inoculated into the vagina at 16.5 dpc, and the cervixes were collected at 17.5 dpc.

Results: The expression of MUC5B/5AC in cervicovaginal fluid was decreased in pregnant women after trachelectomy concomitant with the anatomical loss of cervical glands. Post-trachelectomy women delivered at term when MUC5B/AC abundance was greater than the mean normalized abundance of the control. MUC5B levels in the cervix were increased during pregnancy in both humans and mice. *MUC5B* mRNA was increased by addition of estradiol in human cervical epithelial cells, whereas *MUC5AC* was not. In a pregnant mouse model of ascending infection, *E. coli* was trapped in the MUC5B/AC-expressing mucin of the cervix, and neutrophils were colocalized there.

Conclusion: Endocervical MUC5B and MUC5AC may be barriers to ascending pathogens during pregnancy.

Key Words: cervicovaginal fluid, innate immunity, mucin, mucus, proteomics, trachelectomy

Abbreviations: ANOVA, analysis of variance; CVF, cervicovaginal fluid; DAB, 3,3'-diaminobenzidine; dpc, days postcoitum; PBS, phosphate-buffered saline; PCR, polymerase chain reaction; PPRM, preterm prelabor rupture of membrane.

Preterm birth is a leading cause of perinatal mortality and long-term morbidity (1). Twenty-five percent to 40% of preterm births are attributed to intrauterine infection (1–3), which is mainly caused by ascending microbes from the vagina. However, the underlying protective mechanisms of the cervix are not fully understood, resulting in difficulty predicting and preventing preterm birth.

The uterine cervix plays an essential role in the maintenance of pregnancy, providing a passage between the vagina and the uterus and mechanically supporting the uterine contents. After any cervical excisional surgery, including conization due to cervical lesions, the rate of preterm birth increases by as much as 10% (4–6). Another fertility-sparing surgery, trachelectomy, was first reported in 1987 (7) for the treatment of early invasive cervical cancer. Trachelectomy removes most parts of the cervix and only preserves approximately 5 to 10 mm of the upper endocervix (7–9). As a result, the preterm birth rate of women after trachelectomy reaches more than 50% (10). These preterm births are presumably due to (i)

lack of mechanical support, (ii) impairment of local immunological defense mechanisms, and (iii) alteration of cervicovaginal microbiota (4, 11–13).

Cervicovaginal fluid (CVF) contains a complex mixture of secretions from the cervix (14, 15), including mucus, which is believed to form a barrier against ascending infection (16, 17). The mucus is composed of water and mucins (18–20). Mucins are of 2 types: transmembrane mucins and secreted gel-forming mucins, such as MUC2, MUC5B, MUC5AC, MUC6, and MUC19 (18–21). These secreted gel-forming mucins are highly glycosylated proteins and are physically very large, spanning 0.2 to 10 μm in length for single polymers, interweaving to form mesh-like gels (18, 22). These mucins coat the wet epithelial surface of various human organs, including the airway, gastrointestinal tract, and uterine cervix (17–20), and establish innate immunity to prevent bacterial invasion (23, 24). Therefore, we hypothesized that the analysis of CVF from pregnant women after trachelectomy would reveal some aspects of

the preterm-birth mechanism and contribute to finding a novel biomarker of preterm birth.

In this study, we employed both proteomics of CVF and clinical data from pregnant women undergoing trachelectomy to identify preterm birth-related proteins in the cervix and investigated the roles of these cervical proteins in the maintenance of pregnancy through cell culture and a pregnant mouse model.

Materials and Methods

Study 1: A Descriptive Cross-Sectional Study

We performed a descriptive cross-sectional study of pregnant women who had undergone radical trachelectomy whose pregnancy was managed at Kyoto University Hospital (Kyoto, Japan), Kitano Hospital (Osaka, Japan), and Kobe City Medical Center General Hospital (Hyogo, Japan) between January 2013 and March 2021 (Tables S1 and S2 (25)). Maternal background characteristics and perinatal clinical features were obtained from the medical records. To analyze the effect of cervical excision on spontaneous preterm birth, we excluded multifetal pregnancy and iatrogenic preterm birth due to maternal complications, such as hypertensive disorders, or fetal complications, such as severe growth restriction or nonreassuring fetal status. Cases of pregnancy loss before 22 weeks of gestation were also excluded from this study. We examined the correlation between residual cervical length at 18 to 22 weeks of gestation and gestational age at delivery in pregnancy after radical trachelectomy. The cervical length was measured at every prenatal visit (2-4 visits between 18 and 22 weeks of gestation), and the mean cervical length was used in this analysis. We also analyzed the association between the Nugent score and preterm birth. The maximum second-trimester Nugent score was chosen for this analysis.

Study 2: A Case-Control Study for CVF Proteomic Analysis

We also performed a case-control study for CVF proteomic analysis of pregnant women at Kyoto University Hospital and 10 affiliated hospitals from January 2018 to March 2020 (Table S1 (25)). CVF samples were collected once between 18 and 24 weeks of gestation. At the time of sampling, we excluded cases who had had unprotected sexual intercourse in the preceding 48 hours or cases with vaginal bleeding in the preceding 24 hours to avoid distortion of the aligned total protein of each sample in liquid chromatography-tandem mass spectrometry analysis due to contamination by semen or blood. From the collected samples, a case-control group was selected for CVF proteomic analysis. The case group (post-trache) consisted of 8 pregnant women who had undergone radical trachelectomy before pregnancy. The control group consisted of 10 pregnant women selected randomly from the uncomplicated pregnant women without a surgical history who delivered vaginally at term. All 8 women in the post-trache group overlapped with Study 1 (cases 14, 17-22, and 24 in Table S1 (25)). Exclusion criteria for the study were multifetal pregnancy and iatrogenic preterm birth due to maternal complications, such as hypertensive disorders, or fetal complications, such as severe growth restriction or nonreassuring fetal status. None of the CVF swabs were macroscopically contaminated with blood.

CVF Sample Collection

A cotton swab was inserted into the posterior fornix of the vagina and kept in place for 6 seconds. Next, the swab was swirled

in a 2 mL tube containing 1.5 mL of phosphate-buffered saline (PBS) (Nissui Pharmaceutical, #05913, Dulbecco PBS (-)). The tube was then immediately stored at -20°C until transportation to our laboratory for storage at -80°C until processing.

Liquid Chromatography-Tandem Mass Spectrometry and Label-free Relative Quantification

Frozen CVF samples were thawed at room temperature and centrifuged at 15 000g for 10 minutes at 4°C . Supernatants were collected, and their protein concentrations were determined by a Pierce BCA Protein Assay Kit (#23227, Thermo Fisher Scientific). Eight micrograms of protein was precipitated by ice-cold acetone and resuspended in 8 M urea/30 mM ammonium bicarbonate. The proteins were digested with trypsin, purified by a Pierce C18 spin column (#89870, Thermo Fisher Scientific), and resuspended in 0.1% formic acid. One microgram of digested protein was separated using Nano-LC-Ultra 2D-plus (Eksigent) with a trap column (200 $\mu\text{m} \times 0.5 \text{ mm}$ ChromXP C18-CL 3 μm 120 \AA [Eksigent]) and an analytical column (75 $\mu\text{m} \times 15 \text{ cm}$ ChromXP C18-CL 3 μm 120 \AA [Eksigent]). Solvents A and B were 0.1% formic acid/water and 0.1% formic acid/acetonitrile, respectively, and the binary gradient used for the separation was as follows: A98%/B2% to A66.8%/B33.2% for 12.5 minutes, A66.8%/B33.2% to A2%/B98% for 2 minutes, A2%/B98% for 5 minutes, A2%/B98% to A98%/B2% for 0.1 minute, and A98%/B2% for 17.9 minutes. The flow rate was 300 nL/minute, and the analytical column temperature was 40°C . The eluates were directly infused into a mass spectrometer (TripleTOF 5600+ System [SCIEX]) and ionized in electrospray ionization-positive mode. Data acquisition was carried out with an information-dependent acquisition method (26). The acquired datasets were analyzed using ProteinPilot software version 5.0.1 (SCIEX) for peptide and protein identification, with the UniProtKB/Swiss-Prot database for humans (April 2020) appended to the known common contaminants database (SCIEX). The reliability of the peptide identification was evaluated by the confidence scores calculated by ProteinPilot, and the quality of the database search was confirmed by false discovery rate analysis in which the reversed amino acid sequences were used as decoys. The relative abundances of the identified proteins were estimated on Progenesis QI for Proteomics software version 4.2 (Nonlinear Dynamics, Newcastle upon Tyne, UK). Raw data files were imported to generate an aggregate, and the peptide identification results by ProteinPilot with a confidence of at least 95% were used for the analysis. Label-free quantification of proteins was performed using the Hi-N method employing protein grouping (Nonlinear Dynamics) (27). Proteins with an expression change greater than 1.5-fold and a *P* value (analysis of variance [ANOVA] test) less than .05 were considered differentially expressed proteins.

Gene Ontology Analysis

Gene Ontology analysis was performed by the online analysis database Enrichr (<https://maayanlab.cloud/Enrichr/>). We analyzed 48 proteins that were significantly different between pregnant women after trachelectomy (post-trache) and control pregnant women (Study 2) as determined by CVF proteomics.

Immunohistochemical Analysis of the Uterus and Cervix

We analyzed hysterectomy cases from 6 pregnant women and 4 nonpregnant women after radical trachelectomy and compared them with those of 9 nonpregnant women who had no history of cervical surgery at Kyoto University Hospital (Table S3 (25)). Mid-sagittal uterine sections were fixed in 10% formalin and paraffin embedded. Murine cervixes were collected from nonpregnant and pregnant mice at the indicated times after washing with PBS and were then fixed with 4% paraformaldehyde overnight and kept in 70% ethanol until paraffin embedding.

Paraffin-embedded human and murine specimens were cut into 3- to 4- μ m-thick sections. The tissue sections were deparaffinized, and antigen retrieval was performed in 10 mM sodium citrate buffer (pH 6.0) in a microwave for 20 minutes. Endogenous peroxidase activity was blocked with 3% H₂O₂. These sections were incubated with rabbit polyclonal antibody against MUC5B (Novus Biologicals, #NBP1-92151, RRID:AB467559, 1:500) or mouse monoclonal antibody against MUC5AC (Novus Biologicals, #NBP2-15196, RRID:AB2894883, 1:100) overnight at 4 °C, followed by incubation with biotinylated goat antirabbit or rabbit antimouse secondary antibody (#424032 or #424022, Nichirei) at room temperature for 30 minutes. Then, the samples were incubated with streptavidin-peroxidase complex solution (#424032 or #424022, Nichirei) for 30 minutes. Peroxidase activity was visualized by treatment with 3,3'-diaminobenzidine (DAB). The sections were counterstained with hematoxylin. All images of the immunohistochemical stained sections were obtained with an all-in-one fluorescence microscope (BZ-X800; KEYENCE). Positive areas of DAB staining in the whole human cervix were automatically calculated at 40 \times magnification using BZ-X Analyzer software (KEYENCE) as described previously (28, 29). The areas of cervical glands were measured by QuPath 0.2.3 (30) at 100 \times magnification from 5 randomly selected fields, and the average was used for analysis. Positive areas of DAB staining in the murine cervix were counted at 200 \times magnification from 3 randomly selected fields, and the average areas were calculated.

Immunocytochemistry

Immunocytochemistry staining of human endocervical epithelial cells was conducted as described previously (31). The primary antibodies used were as follows: E-cadherin (Cell Signaling, #14472, RRID:AB2728770, 1:100), vimentin (Cell Signaling, #5741, RRID:AB10695459, 1:200), CK18 (BioLegend, #628401, RRID:AB439770, 1:250), and CK14 (BioLegend, #905303, RRID:AB2734678, 1:500). E-cadherin (epithelial marker) and vimentin (mesenchymal marker) antibodies were used to confirm that the isolated cells were epithelial cells. CK14 (endocervical marker) and CK18 (ectocervical marker) antibodies were used to confirm that the isolated cells were endocervical, not ectocervical, cells (32).

Isolation and Culture of Human Endocervical Epithelial Cells

Cervical tissues were obtained from nonpregnant premenopausal women undergoing hysterectomy. Separation and isolation of human endocervical epithelial cells were performed as previously described (32). Briefly, epithelial tissue was dissected from the endocervix of the tissue sample. The tissue was

digested overnight at 4 °C in keratinocyte basal medium 2 (PromoCell, #C-20211) with 25 units/mL dispase (Thermo Fisher Scientific #17105041). The next day, the surface epithelium from the tissue was scraped off and placed in keratinocyte basal medium 2 with 0.2% trypsin for 10 minutes at 4 °C. Samples were then transferred to a 37 °C water bath and incubated for 30 minutes. After centrifugation at 200g for 10 minutes, cells were seeded on 12-well collagen-type I-coated microplates with a lid at 2×10^4 cells/cm² (#4815-010, IWAKI). Isolated cells were cultured in keratinocyte growth medium 2 (#D-12001, PromoCell) with 5% fetal bovine serum, 100 U/mL penicillin, and 100 μ g/mL streptomycin (#2625384, Nacalai Tesque) and cultured in 5% CO₂ and 95% air at 37 °C. Two days after plating, the primary cultured cells were treated with the indicated dose of progesterone (100 nM, #2892164 Nacalai Tesque), estradiol (10 nM, #E7376, LKT laboratories), or combined progesterone and estradiol (100 and 10 nM, respectively) for 24 hours. Steroids were dissolved in DMSO (#13408-64, Nacalai Tesque). Subculture of isolated primary cells was not performed.

Pregnant Mouse Model

Eight- to ten-week-old C57BL/6J wild-type nonpregnant mice and 10- to 12-week-old pregnant mice were purchased from SLC Japan. The whole cervix was collected from nonpregnant and pregnant mice at 10.5, 13.5, and 16.5 days postcoitum (dpc) after washing with PBS and was then quickly frozen in liquid nitrogen and stored at -80 °C. The cervixes were otherwise fixed with 4% paraformaldehyde overnight and kept in 70% ethanol until paraffin embedding for histology.

Mouse Model of Ascending Infection by Vaginal *Escherichia coli* Inoculation

Mouse ascending infection by vaginal *E. coli* inoculation was induced by the method published by Akgul et al with slight modifications (33, 34). Briefly, at 16.5 dpc, pregnant mice were anesthetized with isoflurane and received either live *E. coli* (serotype O55; ATCC) (20 μ L bacteria equal to 10^4 CFU) or PBS (20 μ L) transvaginally using a 200- μ L pipette. Eight mice were randomly assigned to each group (n = 4). These mice were sacrificed 24 hours after vaginal inoculation for cervical tissue collection. The cervixes were fixed with 4% paraformaldehyde overnight and kept in 70% ethanol until paraffin embedding for histology. Dose determination for *E. coli* inoculation was conducted as described previously (34). The same experiment was conducted a second time to provide fresh frozen cervix to isolate RNA for quantitative real-time polymerase chain reaction (PCR).

Immunofluorescence Staining of the Cervix in the Mouse Model

Immunofluorescence staining was conducted as described previously (35). Antigen retrieval was performed by incubation with proteinase K (P8107S; New England Biolabs; working concentration, 0.6 U/mL) for rabbit polyclonal antibodies against *E. coli* (#ab137967 Abcam, RRID:AB2917966, 1:500) and Ly6G (#14-5931-82, eBioscience, RRID:AB467730, 1:100); antigen retrieval was performed in 10 mM sodium citrate buffer (pH 6.0) in a microwave for antibodies against MUC5B and MUC5AC. Images were taken by an all-in-one fluorescence microscope (BZ-X800; KEYENCE).

Ly6G-positive cells on the mucins in the cervical canal were automatically calculated at 400× magnification using BZ-X analyzer software as described above.

RNA Isolation and Quantitative Real-time PCR

Total RNA was extracted from human endocervical epithelial cell cultures and murine whole cervical tissues using a PureLink RNA mini kit (#12183020, Invitrogen). Reverse transcription of RNA was performed using ReverTra Ace (#TRT-101 m Toyobo Life Science). Primer sequences are shown elsewhere (Table S4 (25)). Quantitative real-time PCR was performed using Thunderbird Next SYBR qPCR mix (#QPS-201, TOYOBO Life Science) on the StepOnePlus (Thermo Fisher Scientific). The results were analyzed using the delta–delta cycle threshold approach with *GAPDH* as the human endogenous control and *Cpha* as the mouse endogenous control.

Ethics

All human studies were approved by the Kyoto University Graduate School of Medicine, Ethics Committee (G0325 and G1149), which deliberates on matters related to ethics in medical research involving human subjects in compliance with various national guidelines and in accordance with the Declaration of Helsinki. Informed consent was obtained to collect CVF for proteomics analysis (Study 2) and to isolate human endocervical cells. We also employed the opt-out method (36) to obtain consent in the descriptive cross-sectional study (Study 1) and immunohistochemical analysis of human uterine specimens.

All animal studies were approved by the Animal Research Committee, Graduate School of Medicine, Kyoto University (MedKyo 21516), which deliberates on the proper conduct of animal experiments.

Statistical Analysis

All normally distributed or non-normally distributed data were expressed as the mean ± SD or median ± interquartile range, respectively. The correlation between the 2 variables was analyzed using Spearman's correlation coefficient. Two categorical independent variables were analyzed by Fisher's exact test. Comparisons between 2 groups were performed using the unpaired *t* test for normally distributed data or the Mann–Whitney *U* test for non-normally distributed data. Comparisons among more than 2 groups were performed using 1-way ANOVA with Dunnett's or Tukey's multiple comparisons test. All statistical analyses were performed using GraphPad Prism 9.2.0 (GraphPad Software). $P < .05$ was regarded as statistically significant.

Result

Study 1: Second-trimester Residual Cervical Length and Nugent Score Were Not Associated With Gestational Age at Delivery in Pregnancy After Trachelectomy

In our descriptive cross-sectional study, 25 pregnancies in 22 women after trachelectomy were analyzed for the relationship between cervical length and gestational age at delivery. Three of these 22 women had a second pregnancy during the study period (cases 14, 24, and 25 in Table S1 (25)). Demographic and birth characteristics are shown elsewhere

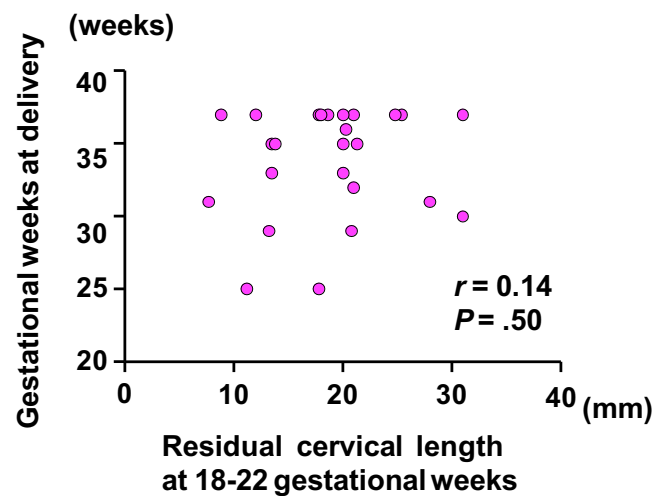


Figure 1. Study 1: Correlation between second-trimester residual cervical length and gestational weeks at delivery in pregnancy after trachelectomy. The dots denote 25 pregnancies in 22 women after trachelectomy surgery, 3 of whom had a second pregnancy during the study period. The correlation was analyzed using Spearman's correlation coefficient.

(Table S2 (25)). The mean gestational age at birth was 33 weeks. The rates of preterm birth and preterm prelabor rupture of membranes (PPROM) were 60% and 52%, respectively. The cervical cerclage placed at the time of the trachelectomy surgery remained throughout pregnancy in all but 2 cases. Interestingly, there was no correlation between residual cervical length at 18–22 weeks of gestation and gestational age at delivery ($r = 0.14$, $P = .50$) (Fig. 1). Next, we analyzed the relationship between preterm birth and Nugent score, which provides gradations of the disturbance of vaginal flora (37). We found that the median Nugent score at the second trimester in 23 pregnancies after trachelectomy (2 cases were missing data) was 1 (interquartile range 0–4, Table S2 (25)), and the Nugent score after trachelectomy was not related to preterm birth (Table 1).

Study 2: MUC5B and MUC5AC Concentrations in CVF Decreased in Pregnancy After Trachelectomy

To identify the risk factors for preterm birth other than cervical length and cervicovaginal bacterial flora, the CVF of 8 pregnant women after trachelectomy (post-trache) and 10 control pregnant women who delivered at term, collected between 18 and 24 weeks of gestation, was analyzed by proteomics (Fig. 2A). The clinical characteristics are shown in Table 2. In the post-trache group, the mean gestational age at birth was 32 weeks, and the PPRM rate was 63%.

Table 1. Nugent score at second-trimester in 23 pregnancies after trachelectomy (Study 1)

Nugent score	Preterm (n = 14)	Term (n = 9)	<i>P</i> value
Normal (≤ 3)	10	7	$> .99^a$
Intermediate or bacterial vaginosis (≥ 4)	4	2	

^aAnalyzed by Fisher's exact test.

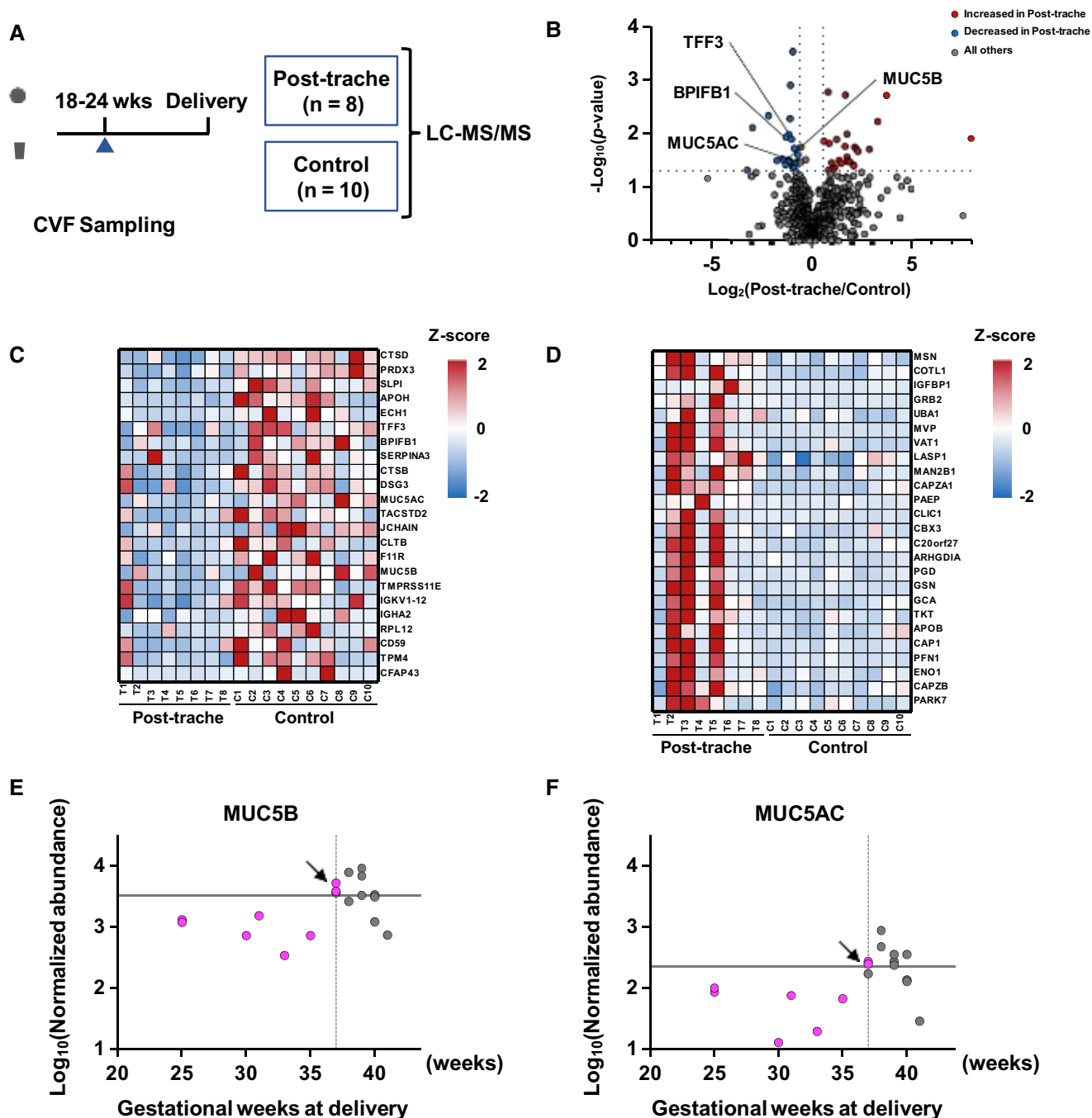


Figure 2. Study 2: Identification and quantification of different CVF proteomic compositions in pregnant women after trachelectomy compared with control pregnant women. (A) Schema of CVF sampling for quantitative proteomic analysis. CVF was collected from pregnant women after trachelectomy (post-trache, n = 8) and term delivery control women without surgical history (control, n = 10). (B) Volcano plot denotes differentially expressed proteins in CVF compared between the 2 groups. The horizontal dotted line shows a P value of .05, and the left and right vertical dashed lines are fold changes (post-trache/control) of 0.67 and 1.5, respectively. Red dots represent 25 significantly increased proteins; blue dots represent 23 significantly decreased proteins in CVFs of women in the post-trache group. Gray dots represent the proteins without differences between the 2 groups. The 4 mucus-associated proteins are labeled. (C, D) Heatmap denotes the specific proteins shown in blue (C) and red (D) dots in the volcano plot. Each column represents a patient, and each row represents a specific protein listed in order of P value from lowest. The color scale represents a z-score of protein expression obtained from each patient, which was converted from the normalized abundance. Blue represents lower expression, and red represents higher expression. (E, F) The scatter plot shows the relationship between the log₁₀-normalized abundance of MUC5B and MUC5AC and gestational age at delivery in all 18 women. Magenta and gray dots represent post-trache and control cases, respectively. The horizontal dotted line shows the mean normalized abundance of the control group, and the vertical dashed line indicates 37 weeks of gestation. The arrows show the same 2 cases in the post-trache group (magenta dots) with MUC5B or MUC5AC abundance beyond the mean normalized abundance of the control. CVF, cervicovaginal fluid.

In CVF proteomics, 601 proteins were commonly quantified in the 2 groups, and 48 differentially secreted proteins were identified between the 2 groups. The expression of 23 proteins

was decreased and the expression of 25 proteins was increased in the CVF of the post-trache group compared with those of the control group (Fig. 2B). Figure 2C and 2D shows the

Table 2. Demographic and birth characteristics of pregnant women after trachelectomy and term delivery controls without surgical history (Study 2)

Demographics	Post-trach (n = 8)	Control (n = 10)	P value
Maternal age, mean ± SD	36.3 ± 3.8	34.2 ± 3.8	.27 ^a
Maternal race, no.			>.99 ^b
Japanese	8	10	
Previous births, no.			>.99 ^b
0	6	7	
1	2	3	
Maternal BMI, kg/m ² , mean ± SD	21.2 ± 3.0	21.6 ± 4.5	.81 ^a
Smoking during pregnancy, No.	0	1	>.99 ^b
Gestational age at CVF sample collection, weeks, mean ± SD	18.6 ± 1.2	19.5 ± 1.6	.21 ^a
Cervical length at 18-22 weeks gestational age, mm, mean ± SD	20.4 ± 7.4	40.6 ± 5.9	<.001 ^a
Gestational age at delivery, weeks, mean ± SD	31.6 ± 4.8	39.1 ± 1.2	<.001 ^a
Incidence of PPRM, no.	5	0	<.01 ^a

Abbreviations: BMI, body mass index; CVF, cervicovaginal fluid; post-trach, pregnant women after trachelectomy; PPRM, preterm prelabor rupture of membranes.

^aAnalyzed by unpaired t test.

^bAnalyzed by Fisher's exact test.

relative abundance of the differentially expressed proteins in each case. Except for insulin-like growth factor binding protein-1, the expression of fibronectin, neutrophil elastase, matrix metalloproteinase 8 and 9, vitamin D-binding protein, and interleukin-1 receptor antagonist protein, which are well-known biomarkers of preterm birth and delivery, was not significantly changed between the 2 groups (Fig. S1 (25)). The expression of antimicrobial peptides, such as elafin, neutrophil defensin 1, cathelicidin antimicrobial peptide, lactotransferrin, bactericidal permeability-increasing protein, and S100 calcium-binding protein A7, was not significantly changed, excluding antileukoproteinase (Fig. S1 (25)). Among 23 decreased proteins in CVF proteomics, as many as 4 proteins (ie, MUC5B, MUC5AC, TFF3, and BPIFB1) were mucus-associated proteins (Fig. 2B and 2C). Since mucin proteins have prevented bacterial invasion in other organs, we focused on MUC5B and MUC5AC. The log₁₀-normalized abundance of MUC5B and MUC5AC was plotted against gestational weeks at delivery (Fig. 2E and 2F). All of the women in the post-trache group with MUC5B or MUC5AC abundance greater than the mean normalized abundance of the control delivered at term (Fig. 2E and 2F, arrows), whereas all the women who had lower abundances delivered preterm.

Gene Ontology Analyses of Proteome Data From CVFs

Gene Ontology analyses were performed using 48 differentially secreted proteins identified between the 2 groups in Study 2. The top 3 biological Gene Ontology terms in the biological process enriched in these 48 proteins were related to the immune response mediated by neutrophils (Fig. S2 (25)).

MUC5B and MUC5AC Expression in the Human Cervix During Pregnancy and After Trachelectomy

Following the results of proteomic analysis, we examined MUC5B and MUC5AC expression in the human uterus (Fig. 3A). MUC5B and MUC5AC were ubiquitously expressed in the columnar epithelial cells of the endocervix (Fig. 3B, 3C, 3E, and 3F), and these mucins filled the lumen in both nonpregnant and pregnant women (Fig. 3B, 3C, 3E, and 3F). In contrast, the expression of MUC5B and MUC5AC was not observed in the endometrium (decidua) or vagina (Fig. 3B, 3C, 3E, and 3F). The cervical gland area was enlarged during pregnancy compared with the nonpregnant cervical gland area ($P < .001$) (Fig. 3H). The MUC5B-positive area also increased in pregnant women compared with nonpregnant women, which corresponded with the dilatation of tubular glands ($P < .001$) (Fig. 3I). In contrast, the MUC5AC-positive area was not changed by pregnancy status (Fig. 3J). Therefore, human cervical glands are enlarged in volume by pregnancy, and MUC5B contents are increased, whereas MUC5AC levels are not.

Next, the effect of trachelectomy was analyzed in nonpregnant uteri. Intriguingly, cervical glands were diminished by trachelectomy in nonpregnant women (Fig. 3D and 3G). The MUC5B- and MUC5AC-positive areas were significantly decreased by trachelectomy in nonpregnant women (Fig. 3I and 3J). These data suggested that both MUC5B and MUC5AC secretion would be insufficient in the endocervix of pregnant women after trachelectomy.

Estradiol Regulates the Expression of MUC5B in the Human Endocervix

We investigated the regulatory mechanism of MUC5B and MUC5AC expression in the cervix using primary epithelial cells isolated from the human endocervix. These isolated cells expressed endocervical epithelial cell markers (E-cadherin and cytokeratin 18), and they did not express mesenchymal markers (vimentin) or ectocervical epithelial cell markers (cytokeratin 14) by immunofluorescence, confirming that the cells were derived from endocervical epithelium (Fig. 4A). The physiological dose of estradiol alone (10 nM) or estradiol plus progesterone (10 and 100 nM, respectively) increased MUC5B mRNA by 1.8-fold in endocervical epithelial cells (Fig. 4B), whereas the MUC5AC mRNA level was not regulated by these sex hormones (Fig. 4C).

MUC5B Expression Increased With Advancing Gestational Age in the Mouse Cervix

To investigate the role of mucins in the cervix during pregnancy in vivo, we utilized pregnant mice. Figure 5 shows the changes in mucin expression in the cervix with advancing gestational age. A sample collection image is shown in Fig. 5A. The morphology of cervical glands was flat in nonpregnant mice, and the expression of both MUC5B and MUC5AC was scarce (Fig. 5B and 5F). At 10.5 dpc, MUC5B and MUC5AC appeared in the cervical glands (Fig. 5C and 5G). At 13.5 dpc, ridges were formed in the endocervix, and the superficial monolayer cells in the endocervix were transformed into mucin-containing columnar cells, in which the nuclei were basally placed (Fig. 5D and 5H). At 16.5 dpc, the endocervix was lined by pseudostratified columnar epithelium (Fig. 5E and 5I). As a result, the MUC5B-positive area of the endocervix significantly increased with advancing

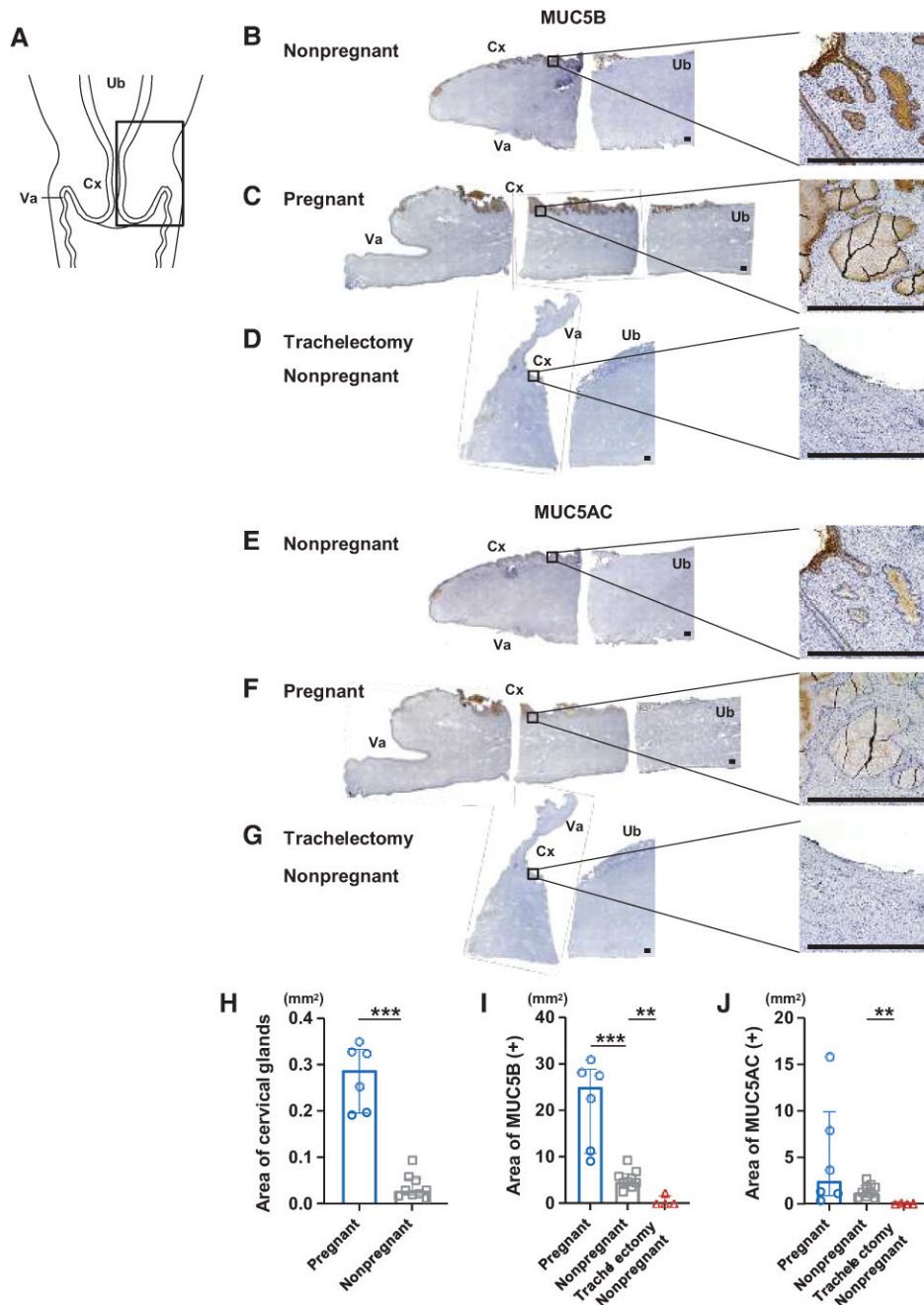


Figure 3. Localization and quantification of MUC5B and MUC5AC in the human uterus during pregnancy and after trachelectomy. (A) Schema of uterine section. (B-G) Representative MUC5B and MUC5AC expression in the human uterus. Right panels are magnified images. A nonpregnant woman (B and E), a pregnant woman at 35 weeks of gestation (C and F), and a nonpregnant woman after trachelectomy (D and G). (H) The areas of cervical glands in 6 normal pregnant women compared with those in 9 nonpregnant women. (I and J) Quantification of MUC5B- and MUC5AC-positive areas in 6 normal pregnant women and 4 nonpregnant women after trachelectomy compared with those in 9 nonpregnant women. Data are represented as the median \pm interquartile range. ** $P < .01$, *** $P < .001$ using a 2-tailed Mann-Whitney U test. Cx, cervix; Ub, uterine body; Va, vagina; Scale bars, 1 mm.

gestational age (Fig. 5J), and MUC5AC expression modestly increased by 16.5 dpc (Fig. 5K), reflecting the tall mucin-filled cytoplasm of each endocervical epithelial cell during pregnancy.

Next, cervical tissues were collected from nonpregnant and pregnant mice at 10.5, 13.5, and 16.5 dpc, and *Muc5b* and *Muc5ac* mRNA expression was analyzed. *Muc5b* mRNA expression in the cervix was very low in nonpregnant mice but increased 150-fold at 10.5 dpc and further increased toward term (Fig. 5L). *Muc5ac* mRNA levels were also low in nonpregnant

mice but increased 40-fold at 10.5 dpc (Fig. 5M). *Muc5ac* mRNA expression gradually decreased with advancing gestational age (Fig. 5M). Collectively, MUC5B was robustly induced in the cervical epithelium by pregnancy in mice as in humans.

MUC5B and MUC5AC Trap the Ascending Bacteria in the Cervical Canal During Pregnancy

Finally, we utilized a pregnant mouse model of ascending infection by *E. coli* (33, 38, 39) to investigate the role of mucin

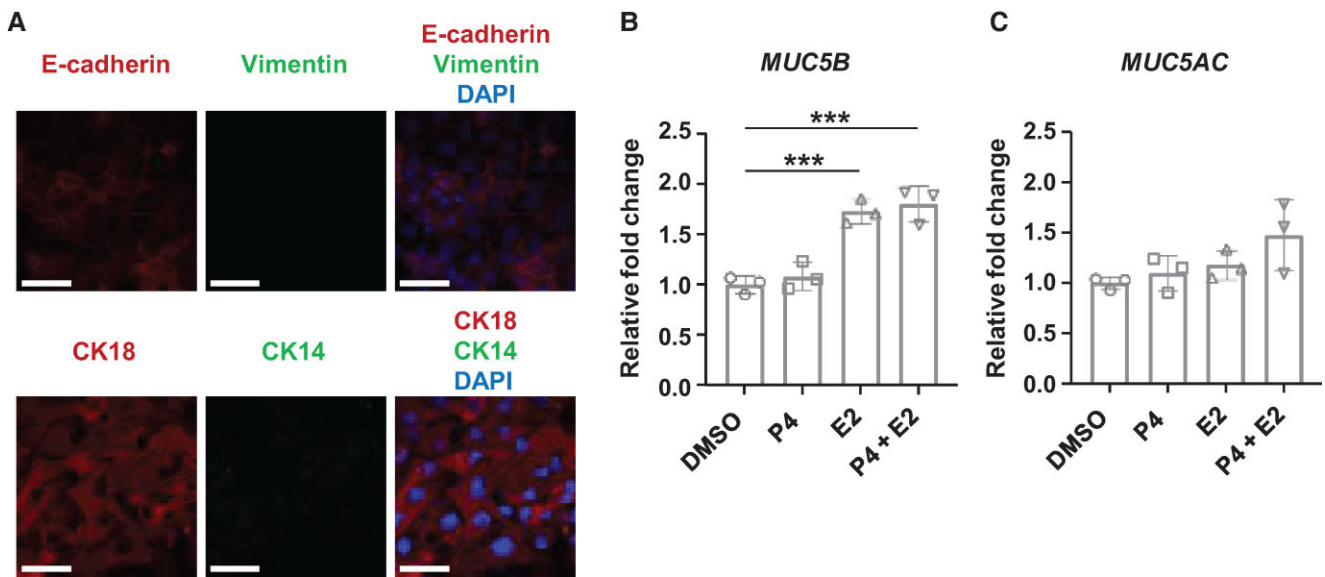


Figure 4. Regulation of MUC5B and MUC5AC in primary epithelial cells isolated from the human endocervix. (A) Representative immunofluorescence for E-cadherin, vimentin, and DAPI (upper panels) and CK18, CK14, and DAPI (lower panels) of the primary epithelial cells isolated from the human endocervix. (B, C) Changes in the mRNA expression of *MUC5B* and *MUC5AC* by estradiol and progesterone. Primary human endocervical epithelial cells were treated with estradiol (10 nM) and progesterone (100 nM) at physiological concentrations during pregnancy. Data are represented as the mean \pm SD from 3 biological replicate experiments. *** P < .001 using ANOVA with Dunnett's multiple comparisons test. E2, estradiol; CK, cytokeratin; P4, progesterone; Scale bars, 50 μ m.

in the cervical barrier against ascending pathogens. *E. coli* or PBS was inoculated into the vagina at 16.5 dpc, and the cervixes were collected after 24 hours at 17.5 dpc (Fig. 6A). Intravaginal *E. coli* inoculation did not cause preterm delivery within 24 hours. Immunofluorescence staining showed that MUC5B and MUC5AC were localized in the cervical canal of all mice (Fig. 6B and 6C). Using an *Escherichia coli*-specific antibody, *E. coli* was observed in the cervical MUC5B- and MUC5AC-expressing mucin in 3 of 4 *E. coli*-inoculated mice (E1, E2, and E3 mice but not the E4 mouse; Fig. 6C and 6E). Furthermore, Ly6G-positive neutrophils were colocalized on these mucins as they were stuck in the mesh-like structure of mucins (Fig. 6C and 6E). Migration of neutrophils was rarely observed in the PBS-treated control but was observed in all *E. coli*-inoculated mice (Fig. 6B-E). Ly6G-positive cell counts on mucins in the cervical canal were significantly increased in *E. coli*-treated mice compared with those in PBS-treated mice ($P = .029$) (Fig. 6G).

Tnf, *Il1b*, *Muc5b*, and *Muc5ac* mRNA expression in the cervix was also measured to determine the cervical and neutrophil response to ascending pathogens. *Tnf* mRNA expression increased 16-fold ($P = .015$), and *Il1b* mRNA expression was not changed by *E. coli* challenge (Fig. 6H and 6I). *Muc5b* mRNA expression increased 1.7-fold (Fig. 6J, $P = .001$), whereas *Muc5ac* mRNA expression was not changed (Fig. 6K). These results suggest that MUC5B in the cervix is not only expressed constitutively during pregnancy but is also induced by external stimuli such as *E. coli* infection.

Discussion

Here, using clinical data and proteomic analysis of CVF in pregnant women who underwent trachelectomy, we reveal that MUC5B and MUC5AC in the cervix probably play a pivotal role in the maintenance of pregnancy. Pregnancy increased

MUC5B expression in the endocervix of both humans and mice. Furthermore, using the mouse model of ascending infection, MUC5B and MUC5AC in the pregnant cervix appear to have a barrier function against microbial invasion.

It has been proposed that the risks of preterm birth in pregnancy after cervical excisional surgeries are the result of a lack of mechanical support by the cervix or alteration of the cervicovaginal microbiota. In this study, we revealed that the residual cervical length and the Nugent score in the second trimester were not correlated with gestational weeks at delivery in post-trachelectomy women. Another study showed only a weak correlation between the second-trimester cervical length and gestational age at delivery after trachelectomy (40), and prophylactic cervical cerclage, which operatively closes and elongates the cervix, is ineffective in preventing preterm birth in pregnant women after cervical excision (41, 42). In addition, metatranscriptomics showed that surgical excision of the cervix did not change the vaginal microbiota composition (43). An association between viscoelasticity or permeability of the whole mucus and preterm birth has been reported (44, 45). These findings suggest that impairment of local immunological defense mechanisms contributes to increased preterm birth and PPRM rates in pregnant women after trachelectomy.

We identified MUC5B and MUC5AC by proteomics as candidate proteins for barriers against pathogens in the cervix. Conditional hyaluronan knockout mice that lost hyaluronan expression in the cervix were more prone to preterm birth (33). These mice also have decreased expression of *Muc5b* in the cervix (more than half of that in wild-type mice) (33). Cervical epithelial damage induced by spermicide, which presumably led to a reduction in mucins, promoted ascending infection in mice and resulted in preterm birth (46). Mucin proteins prevent bacterial invasion into tissues (23, 24). The trap is mediated by carbohydrate interactions in which the sialic acids expressed on mucins bind to bacteria (47, 48). Neutrophils, stuck in the mesh-like structure of cervical

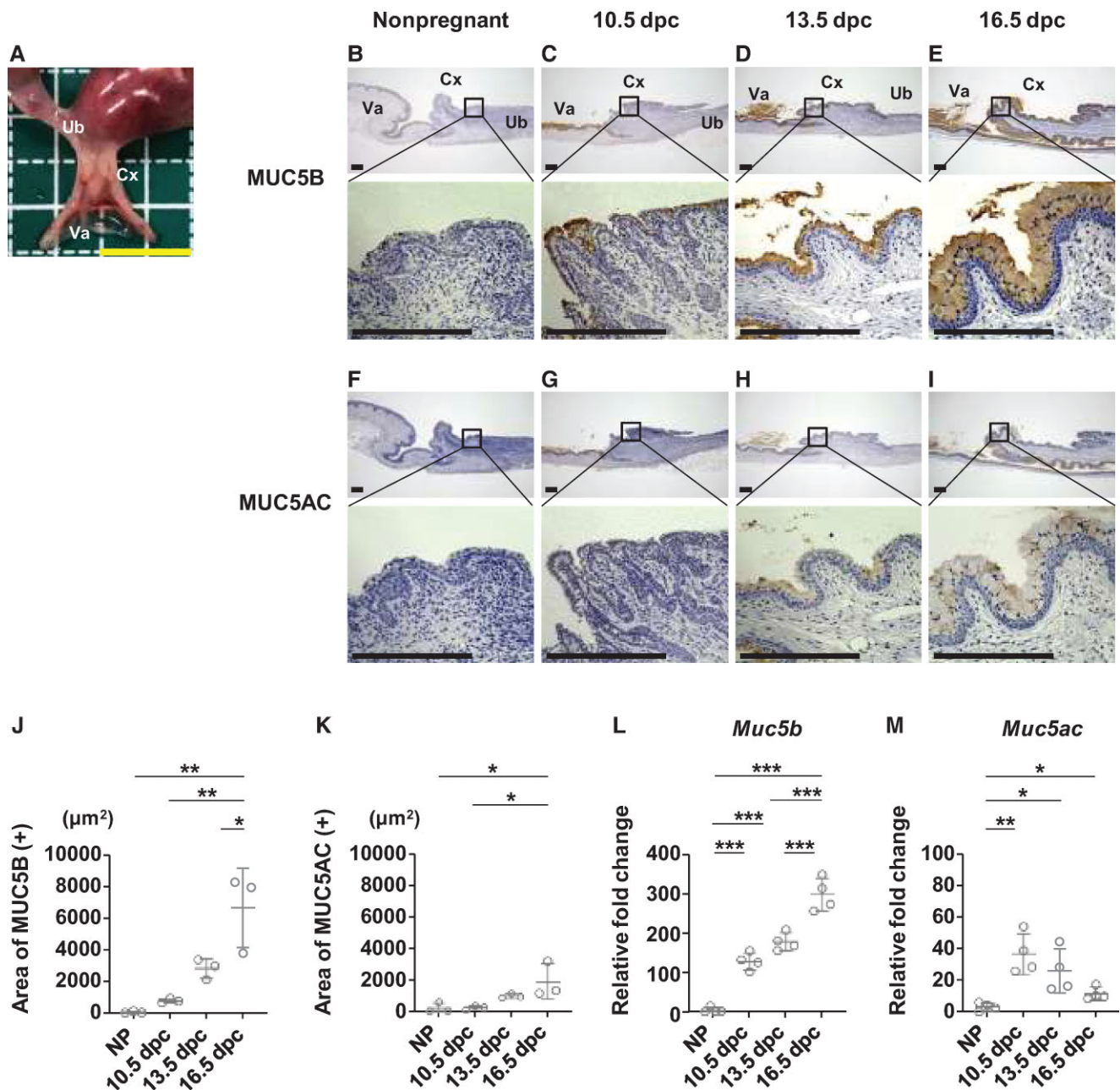


Figure 5. Muc5b and MUC5AC expression in the mouse cervix during pregnancy. (A) Macroscopic view of the pregnant murine vagina and uterus at 16.5 dpc. Scale bars, 10 mm. (B-I) Representative MUC5B and MUC5AC expression on the murine cervix as a function of time by immunohistochemistry. Scale bars, 200 μm. (J, K) Quantification of MUC5B- and MUC5AC-positive areas in the mouse cervix as a function of time. (L, M) Relative mRNA expression levels of *Muc5b* and *Muc5ac* in murine cervixes as a function of time. Data are represented as the means ± SD (n = 3 in J, K and n = 4 in L, M). **P* < .05, ***P* < .01, ****P* < .001 using ANOVA with Tukey’s multiple comparisons test. Cx, cervix; NP, nonpregnant; Ub, uterine body; Va, vagina.

mucins, also bind sialic acids on mucins via L-selectin (49–51). Collectively, MUC5B and MUC5AC in the cervical canal not only trap the ascending bacteria but also provide a scaffold for neutrophils.

We showed that MUC5B content in the cervix was significantly increased by pregnancy in both humans and mice, whereas MUC5AC was not. It has been reported that MUC5B knockout mice are susceptible to airway infection by multiple bacterial species, whereas MUC5AC knockout mice are not (23). Therefore, we suspect that MUC5B may possess more important barrier functions to ascending pathogens than MUC5AC in the cervix during pregnancy.

MUC5B gene expression in human cervical epithelial cells was increased by estradiol, which is synthesized in the placenta and gradually increases in maternal circulation during pregnancy. This is in accordance with previous reports that estradiol increased MUC5B expression in nonpregnant human cervical mucus (17, 52) and human airway epithelial cells (53). Although hyperplasia and dilatation of human cervical glands occur during pregnancy in response to progesterone (54), progesterone did not regulate MUC5B expression in human cervical epithelial cells. It is unclear how *Muc5b* expression is upregulated while *Muc5ac* is downregulated in murine cervical epithelial cells during pregnancy. *Muc5ac* knockout mice showed compensatory upregulation of *Muc5b* in fornical conjunctival epithelia (55).

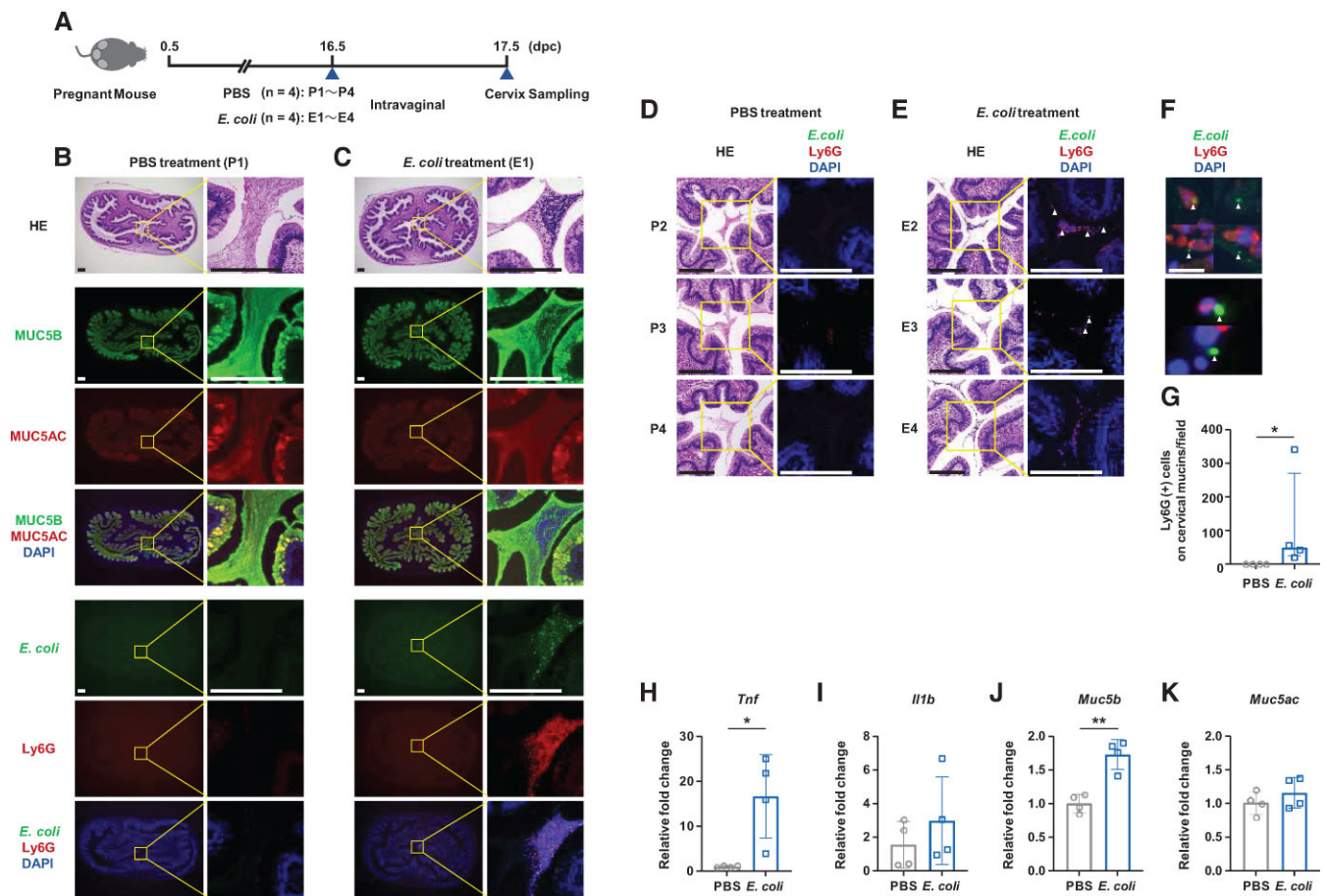


Figure 6. Localization of *Escherichia coli*, neutrophils, and mucins in the cervical canal of a pregnant mouse model of ascending infection. (A) A schematic illustration of the experimental design. (B and C) Hematoxylin and eosin (H&E) and immunofluorescence staining for MUC5B, MUC5AC, *E. coli*, and Ly6G on an axial section of murine cervix. Representative images of mice treated with PBS (B) (P1 mouse) or *E. coli* (C) (E1 mouse). Scale bars, 200 μ m. (D, E) H&E and immunofluorescence staining for *E. coli* and Ly6G on an axial section of the cervix in other mice. Treatment with PBS (D) (P2, P3, P4 mice) or *E. coli* (E) (E2, E3, E4 mice). The arrowhead represents *E. coli* antigens. Scale bars, 200 μ m. (F) Enlarged views indicated by arrowheads in (E) (E2, E3 mice). Scale bars, 10 μ m. (G) The number of Ly6G-positive cells in the cervical mucins per field. Data are represented as the median \pm interquartile range. * P < .05. Two-tailed Mann–Whitney U tests. (H–K) mRNA expression of *Tnf*, *Il1b*, *Muc5b*, and *Muc5ac* in murine cervixes after *E. coli* treatment. Data are represented as the mean \pm SD. * P < .05, ** P < .01 using a 2-tailed unpaired t test.

In contrast, when *Muc5b* was knocked out, *Muc5ac* was not compensatorily upregulated. Similarly, when *Muc5b* was knocked out in olfactory glands, there was no compensatory upregulation of *Muc5ac* (56). It is likely that the interaction between MUC5B and MUC5AC is complicated.

Our proteomic analysis of CVF did not detect MUC2 or MUC4. MUC2 has been reported to separate bacteria from the colon epithelium (24). MUC2 is not observed in normal endocervical epithelium, although it is often found in adenocarcinoma in situ or invasive adenocarcinoma of the endocervix (57). MUC4 is a transmembrane mucin that is not secreted, so MUC4 was not detected in the cervical mucus plug (58). Therefore, MUC5B and MUC5AC, rather than other mucins, may be necessary for the maintenance of pregnancy.

There are several limitations in this study. First, we could not utilize cervix-specific MUC5B/5AC knockout or knockdown mice, so we could not confirm the cervical functions of MUC5B and MUC5AC. Although we tried to generate cervix-specific knockdown mice using the delivery of shRNAs targeting MUC5B packaged by adeno-associated viral vector serotype 6 into the cervix, the viral vector failed to transduce the epithelial cells of the cervix, despite using previously reported methods (38, 59). Second, the sample size of CVF

from women after trachelectomy was relatively small, and, as such, we could not statistically analyze the correlation between the quantitative value of MUC5B or MUC5AC in CVF and gestational age at delivery. We demonstrated that only 2 cases with a sufficient level of MUC5B or MUC5AC in CVF delivered at term. We need to further increase the sample size to elucidate the significant difference between preterm and term delivery in pregnant women after trachelectomy. Third, we could not fully determine the regulatory mechanism of MUC5AC expression in the cervix. MUC5AC has been recognized as a “response mucin,” the expression of which is regulated by several inflammatory stimuli in respiratory epithelia (23, 60). However, we confirmed that lipopolysaccharide did not induce MUC5AC expression in the cell culture from the human endocervix and that vaginal *E. coli* inoculation did not increase MUC5AC expression in the mouse cervix. MUC5AC may be expressed constitutively rather than being inducible by external stimuli in the pregnant cervix as opposed to the respiratory tract.

In conclusion, endocervical MUC5B increases during pregnancy. This cervical mucin, together with MUC5AC, may work as a barrier to ascending pathogens during pregnancy, resulting in the avoidance of preterm birth. In addition to

several challenges in predicting and preventing preterm birth (61, 62), the quantification of MUC5B or MUC5AC in CVF samples may provide a biomarker of preterm birth in the future.

Acknowledgments

We thank Yumi Onishi, Asami Ikeda, Atsuko Taga, Akiko Okuda, and Toshihiro Higuchi (Kitano Hospital, Department of Obstetrics and Gynecology) and Ayami Koike and Shinya Yoshioka (Kobe City Medical Center General Hospital, Department of Obstetrics and Gynecology) for collection of clinical data and CVF samples of pregnant women after trachelectomy. We thank Hiroshi Takai (Japan Baptist Hospital, Department of Obstetrics and Gynecology) for cervical tissue samples. We thank Mizuho Takemura and Ayako Yoshida for technical support and Iku Sugiyama for editorial assistance. We thank Yoshihiro Ishida (Kyoto University Graduate School of Medicine, Department of Dermatology) for technical advice on the isolation and culture of human endocervical epithelial cells. We thank Yucel Akgul (University of Texas, Southwestern Medical Center, Department of Obstetrics and Gynecology) for the *E. coli* inoculation protocol. We thank the shared resource cores in the Medical Research Support Center, Graduate School of Medicine, Kyoto University. We thank the Center for Anatomical, Pathological and Forensic Medical Research, Kyoto University Graduate School of Medicine, for preparing microscope slides. We thank Professor Satoshi Morita for helpful advice on the statistical analysis.

Funding

This work was supported by the Japan Society for the Promotion of Science KAKENHI (grant no. 21K09540, 19K22686, 18K09259), JST SPRING (grant no. JPMJSP 2110) and the Kyoto University 125th Anniversary Fund Kusunoki 125.

Disclosures

The authors declare they have no conflicts of interest and no competing financial interests.

Data Availability

All data are contained within the manuscript. Information of antibodies was obtained by Research Resource Identifier (RRID) (<https://scicrunch.org/resources>). MUC5B, RRID:AB 11019602, http://antibodyregistry.org/AB_11019602. MUC5AC, RRID:AB 2894883, http://antibodyregistry.org/AB_2894883. E-Cadherin, RRID:AB 2728770, http://antibodyregistry.org/AB_2728770. Vimentin, RRID:AB 10695459, http://antibodyregistry.org/AB_10695459. CK 18, RRID:AB 439770, http://antibodyregistry.org/AB_439770. CK 14, RRID:AB 2734678, http://antibodyregistry.org/AB_2734678. *E. coli*, RRID:AB 2917966, http://antibodyregistry.org/AB_2917966. Ly6G, RRID:AB 467730, http://antibodyregistry.org/AB_467730.

References

1. Goldenberg RL, Culhane JF, Iams JD, Romero R. Epidemiology and causes of preterm birth. *Lancet*. 2008;371(9606):75-84.
2. Lettieri L, Vintzileos AM, Rodis JF, Albini SM, Salafia CM. Does "idiopathic" preterm labor resulting in preterm birth exist? *Am J Obstet Gynecol*. 1993;168(5):1480-1485.
3. Romero R, Dey SK, Fisher SJ. Preterm labor: one syndrome, many causes. *Science*. 2014;345(6198):760-765.
4. Sadler L, Saftlas A, Wang WQ, Exeter M, Whittaker J, McCowan L. Treatment for cervical intraepithelial neoplasia and risk of preterm delivery. *JAMA*. 2004;291(17):2100-2106.
5. Kyrgiou M, Koliopoulos G, Martin-Hirsch P, Arbyn M, Prendiville W, Paraskevaides E. Obstetric outcomes after conservative treatment for intraepithelial or early invasive cervical lesions: systematic review and meta-analysis. *Lancet*. 2006;367(9509):489-498.
6. Kyrgiou M, Athanasiou A, Kalliala IEJ, et al. Obstetric outcomes after conservative treatment for cervical intraepithelial lesions and early invasive disease. *Cochrane Database Syst Rev*. 2017;11:CD012847.
7. Dargent D, Martin X, Sacchetoni A, Mathevet P. Laparoscopic vaginal radical trachelectomy: a treatment to preserve the fertility of cervical carcinoma patients. *Cancer*. 2000;88(8):1877-1882.
8. Abu-Rustum NR, Sonoda Y, Black D, Levine DA, Chi DS, Barakat RR. Fertility-sparing radical abdominal trachelectomy for cervical carcinoma: technique and review of the literature. *Gynecol Oncol*. 2006;103(3):807-813.
9. Cohen PA, Jhingran A, Oaknin A, Denny L. Cervical cancer. *Lancet*. 2019;393(10167):169-182.
10. Bentivegna E, Maulard A, Pautier P, Chargari C, Gouy S, Morice P. Fertility results and pregnancy outcomes after conservative treatment of cervical cancer: a systematic review of the literature. *Fertil Steril*. 2016;106(5):1195-1211.e5.
11. Poon LC, Savvas M, Zamblera D, Skyfta E, Nicolaides KH. Large loop excision of transformation zone and cervical length in the prediction of spontaneous preterm delivery. *BJOG*. 2012;119(6):692-698.
12. Stock SJ, Norman JE. Treatments for precursors of cervical cancer and preterm labour. *BJOG*. 2012;119(6):647-649.
13. Sasieni P, Castanon A, Landy R, et al. Risk of preterm birth following surgical treatment for cervical disease: executive summary of a recent symposium. *BJOG*. 2016;123(9):1426-1429.
14. Huggins GR, Preti G. Vaginal odors and secretions. *Clin Obstet Gynecol*. 1981;24(2):355-377.
15. Dasari S, Pereira L, Reddy AP, et al. Comprehensive proteomic analysis of human cervical-vaginal fluid. *J Proteome Res*. 2007;6(4):1258-1268.
16. Becher N, Adams Waldorf K, Hein M, Ulbjerg N. The cervical mucus plug: structured review of the literature. *Acta Obstet Gynecol Scand*. 2009;88(5):502-513.
17. Lacroix G, Gouyer V, Gottrand F, Desseyn J-L. The cervicovaginal mucus barrier. *Int J Mol Sci*. 2020;21(21):8266.
18. Taherali F, Varum F, Basit AW. A slippery slope: on the origin, role and physiology of mucus. *Adv Drug Deliv Rev*. 2018;124:16-33.
19. Demouveau B, Gouyer V, Gottrand F, Narita T, Desseyn JL. Gel-forming mucin interactome drives mucus viscoelasticity. *Adv Colloid Interface Sci*. 2018;252:69-82.
20. Wagner CE, Wheeler KM, Ribbeck K. Mucins and their role in shaping the functions of mucus barriers. *Annu Rev Cell Dev Biol*. 2018;34:189-215.
21. Hansson GC. Mucins and the microbiome. *Annu Rev Biochem*. 2020;89:769-793.
22. Boucher RC. Muco-obstructive lung diseases. *N Engl J Med*. 2019;380(20):1941-1953.
23. Roy MG, Livraghi-Butrico A, Fletcher AA, et al. Muc5b is required for airway defence. *Nature*. 2014;505(7483):412-416.
24. Johansson ME, Phillipson M, Petersson J, Velcich A, Holm L, Hansson GC. The inner of the two Muc2 mucin-dependent mucus layers in colon is devoid of bacteria. *Proc Natl Acad Sci U S A*. 2008;105(39):15064-15069.
25. Ueda Y, Mogami H, Kawamura Y, et al. Supplemental materials: cervical MUC5B and MUC5AC are barriers to ascending

- pathogens during pregnancy. Kyoto University Research Information Repository (KURENAI). Deposited August 18, 2022.
26. Andrews GL, Simons BL, Young JB, Hawkrigde AM, Muddiman DC. Performance characteristics of a new hybrid quadrupole time-of-flight tandem mass spectrometer (TripleTOF 5600). *Anal Chem*. 2011;83(13):5442-5446.
 27. Silva JC, Gorenstein MV, Li GZ, Vissers JP, Geromanos SJ. Absolute quantification of proteins by LCMSE: a virtue of parallel MS acquisition. *Mol Cell Proteomics*. 2006;5(1):144-156.
 28. Ohuchi K, Fujimura T, Lyu CB, Amagai R, Muto Y, Aiba S. Possible roles of CXCL13/CXCR5 axis in the development of bullous pemphigoid. *J Dermatol*. 2021;48(3):353-359.
 29. Ukita M, Hamanishi J, Yoshitomi H, et al. CXCL13-producing CD4+ T cells accumulate in early phase of tertiary lymphoid structures in ovarian cancer. *JCI Insight*. 2022;7(12):e157215.
 30. Bankhead P, Loughrey MB, Fernández JA, et al. Qupath: open source software for digital pathology image analysis. *Sci Rep*. 2017;7(1):16878.
 31. Mogami H, Hari Kishore A, Akgul Y, Word RA. Healing of preterm ruptured fetal membranes. *Sci Rep*. 2017;7(1):13139.
 32. Deng H, Mondal S, Sur S, Woodworth CD. Establishment and optimization of epithelial cell cultures from human ectocervix, transformation zone, and endocervix optimization of epithelial cell cultures. *J Cell Physiol*. 2019;234(6):7683-7694.
 33. Akgul Y, Word RA, Ensign LM, et al. Hyaluronan in cervical epithelia protects against infection-mediated preterm birth. *J Clin Invest*. 2014;124(12):5481-5489.
 34. Akgul Y, Mahendroo M. Assessment of changes in the peripartum cervix. In *The Guide to Investigation of Mouse Pregnancy*. Academic Press; 2014:723-731.
 35. Kiyokawa H, Mogami H, Ueda Y, et al. Maternal glucocorticoids make the fetal membrane thinner: involvement of amniotic macrophages. *Endocrinology*. 2019;160(4):925-937.
 36. Clark AM, Jamieson R, Findlay IN. Registries and informed consent. *N Engl J Med*. 2004;351(6):612-614; author reply 612-614.
 37. Nugent RP, Krohn MA, Hillier SL. Reliability of diagnosing bacterial vaginosis is improved by a standardized method of gram stain interpretation. *J Clin Microbiol*. 1991;29(2):297-301.
 38. Suff N, Karda R, Diaz JA, et al. Ascending vaginal infection using bioluminescent bacteria evokes intrauterine inflammation, preterm birth, and neonatal brain injury in pregnant mice. *Am J Pathol*. 2018;188(10):2164-2176.
 39. Spencer NR, Radnaa E, Baljinnayam T, et al. Development of a mouse model of ascending infection and preterm birth. *PLoS One*. 2021;16(12):e0260370.
 40. Kasuga Y, Miyakoshi K, Nishio H, et al. Mid-trimester residual cervical length and the risk of preterm birth in pregnancies after abdominal radical trachelectomy: a retrospective analysis. *BJOG*. 2017;124(11):1729-1735.
 41. Grabovac M, Lewis-Mikhael AM, McDonald SD. Interventions to try to prevent preterm birth in women with a history of conization: A systematic review and meta-analyses. *J Obstet Gynaecol Can*. 2019;41(1):76-88.e7.
 42. Cho GJ, Ouh Y-T, Kim LY, et al. Cerclage is associated with the increased risk of preterm birth in women who had cervical conization. *BMC Pregnancy Childbirth*. 2018;18(1):277.
 43. Mitra A, MacIntyre DA, Paraskevasi M, et al. The vaginal microbiota and innate immunity after local excisional treatment for cervical intraepithelial neoplasia. *Genome Med*. 2021;13(1):176.
 44. Critchfield AS, Yao G, Jaishankar A, et al. Cervical mucus properties stratify risk for preterm birth. *PLoS One*. 2013;8(8):e69528.
 45. Smith-Dupont KB, Wagner CE, Witten J, et al. Probing the potential of mucus permeability to signify preterm birth risk. *Sci Rep*. 2017;7(1):10302.
 46. Pavlidis I, Spiller OB, Demarco GS, et al. Cervical epithelial damage promotes *Ureaplasma parvum* ascending infection, intrauterine inflammation and preterm birth induction in mice. *Nat Commun*. 2020;11(1):1-12.
 47. Prakobphol A, Tangemann K, Rosen SD, Hoover CI, Leffler H, Fisher SJ. Separate oligosaccharide determinants mediate interactions of the low-molecular-weight salivary mucin with neutrophils and bacteria. *Biochemistry*. 1999;38(21):6817-6825.
 48. Linden SK, Sutton P, Karlsson NG, Korolik V, McGuckin MA. Mucins in the mucosal barrier to infection. *Mucosal Immunol*. 2008;1(3):183-197.
 49. Kim YJ, Borsig L, Han H-L, Varki NM, Varki A. Distinct selectin ligands on colon carcinoma mucins can mediate pathological interactions among platelets, leukocytes, and endothelium. *Am J Pathol*. 1999;155(2):461-472.
 50. Wahrenbrock M, Borsig L, Le D, Varki N, Varki A. Selectin-mucin interactions as a probable molecular explanation for the association of Trousseau syndrome with mucinous adenocarcinomas. *J Clin Invest*. 2003;112(6):853-862.
 51. Ivetic A, Hoskins Green HL, Hart SJ. L-selectin: a major regulator of leukocyte adhesion, migration and signaling. *Front Immunol*. 2019;10:1068.
 52. Gipson IK, Moccia R, Spurr-Michaud S, et al. The amount of MUC5B mucin in cervical mucus peaks at midcycle. *J Clin Endocrinol Metab*. 2001;86(2):594-600.
 53. Choi HJ, Chung Y-S, Kim HJ, et al. Signal pathway of 17beta-estradiol-induced MUC5B expression in human airway epithelial cells. *Am J Respir Cell Mol Biol*. 2009;40(2):168-178.
 54. Maqueo M, Azuela JC, Calderon JJ, Goldzieher JW. Morphology of cervix in women treated with synthetic progestins. *Am J Obstet Gynecol*. 1966;96(7):994.
 55. Marko CK, Tisdale AS, Spurr-Michaud S, Evans C, Gipson IK. The ocular surface phenotype of Muc5ac and Muc5b null mice. *Invest Ophthalmol Vis Sci*. 2014;55(1):291-300.
 56. Amini SE, Gouyer V, Portal C, Gottrand F, Desseyn JL. Muc5b is mainly expressed and sialylated in the nasal olfactory epithelium whereas Muc5ac is exclusively expressed and fucosylated in the nasal respiratory epithelium. *Histochem Cell Biol*. 2019;152(2):167-174.
 57. Riethdorf L, O'Connell JT, Riethdorf S, Cviko A, Crum CP. Differential expression of MUC2 and MUC5AC in benign and malignant glandular lesions of the cervix uteri. *Virchows Arch*. 2000;437(4):365-371.
 58. Lee D-C, Hassan SS, Romero R, et al. Protein profiling underscores immunological functions of uterine cervical mucus plug in human pregnancy. *J Proteomics*. 2011;74(6):817-828.
 59. Abdel-Motal UM, Harbison C, Han T, et al. Prolonged expression of an anti-HIV-1 gp120 minibody to the female rhesus macaque lower genital tract by AAV gene transfer. *Gene Ther*. 2014;21(9):802-810.
 60. Okuda K, Chen G, Subramani DB, et al. Localization of secretory mucins MUC5AC and MUC5B in normal/healthy human airways. *Am J Respir Crit Care Med*. 2019;199(6):715-727.
 61. Bachkangi P, Taylor AH, Bari M, Maccarrone M, Konje JC. Prediction of preterm labour from a single blood test: the role of the endocannabinoid system in predicting preterm birth in high-risk women. *Eur J Obstet Gynecol Reprod Biol*. 2019;243:1-6.
 62. Di Renzo GC, Tosto V, Tsibizova V, Fonseca E. Prevention of preterm birth with progesterone. *J Clin Med*. 2021;10(19):4511.